Journal of Computational Physics **161,** 558–575 (2000)
doi:10.1006/jcph.2000.6513, available online at http://www.idealibrary.com on IDEAL®

The Spectral Collocation Method for the Kinetic Equation with the Nonlinear Two-Dimensional Coulomb Collisional Operator

Ildar. K. Khabibrakhmanov* and George. V. Khazanov†

**Department of Physics and Engineering Physics, University of Saskatchewan, Saskatoon, Saskatchewan, Canada, S7N 5E2; †Geophysical Institute and Department of Physics, University of Alaska, Fairbanks, Alaska, 99701*
E-mail: ildar@isas62.usask.ca,khazanov@gi.alaska.edu

Received April 2, 1999; revised March 20, 2000

The spectral collocation method is used for numerical solution of the Fokker–Planck equation with nonlinear integro-differential coulomb collisional operator. The spectral collocation method in general gives superior results to the usually employed finite difference method approximation. High order approximation of the integro-differential operator by the spectral collocation is able to provide highly accurate results on sparse grids. Approximation of the boundary conditions of the problem is very straightforward and natural. The method is also capable of easily accounting for the physically important conservation properties of the system. In this article the details of the numerical implementation of the Fokker–Planck equation solver with Coulomb collisional operator are discussed. Some test results are presented and certain limitations of the implementation are discussed. The method is applied to the problem of plasma heating by superthermal radiation. The self-similar solution is obtained for this case.

Key Words: Fokker–Planck equation; spectral collocation; Coulomb collisions.

CONTENTS

1. INTRODUCTION

Detailed knowledge of the charged particle distribution function is very important in many areas of plasma physics. It is quite common in applications to assume that the main

0021-9991/00 $35.00

body of the distribution function is a thermal equilibrium local Maxwellian function. When the deviations of the distribution function from Maxwellian are small an appropriate linearization procedure can be applied. This approach simplifies description of the plasma significantly. Superthermal electrons in the Earth's plasmasphere, for instance, usually are described by including the linearized Coulomb collisional operator [10, 11] where it is assumed that high energy particles are scattered only by the fixed background thermal population. However, in a great number of applications large deviations from local Maxwellian can be developed. For example, in space plasma physics it is common to consider the response of the plasma to the external forces in a collisionless regime. This means that the characteristic times of the processes in the plasma are much shorter than normal collisional times calculated assuming that distributions are local Maxwellian functions. Nevertheless collisions are important on the longer time scales and are capable of completely redefining the stationary state of the plasma. On the other hand the coulomb collisional relaxation rate is well known to be highly sensitive to where in the velocity phase space the deviation from Maxwellian occurs. For example, the response of low energy particles is much faster than relaxation of high energy particles. In fact, the local coulomb relaxation rate is singular at $v = 0$ and thus in a sense for low energy particles the coulomb collision is always a dominant process.

Collisions of the charged particles in plasma are described by a complicated nonlinear (quadratic in distribution function) integro–differential equation [17]. The rate of the collisional relaxation is quite sensitive to the local, in the velocity phase space, deviations of the distribution function from equilibrium Maxwellian. The fine structure of the relaxation often becomes important in application problems. For instance, the particle loss rates of the trapped particles in the fusion devices, or in natural magnetic confinement of the planetary magnetospheres, are very sensitive to the local gradients of the distribution function in the velocity space. It is therefore important to have a tools for the exact description of the Coulomb collision effects.

The finite difference approximation of the full Coulomb collisional operator was developed, for example, in [12]. Special techniques have been developed recently to improve the accuracy of finite difference approximations [1, 2, 5, 6, 18]. The Legendre series expansion, originally proposed in [17] for the reduction of the collisional operator to the form of Fokker–Planck operator, was used to represent the angular dependencies in a spherical system of coordinates in the velocity space. This fact is a main motivation for the implementation of the collisional operator by the spectral collocation method [3, 7]. In addition to being consistent with the Legendre polynomial expansion of expressions for the Fokker–Planck coefficients, the spectral collocation method generally provides superior high order approximation and allows us to obtain highly accurate results on much sparser grids than the finite difference methods. There are of course certain limitations of the method relevant for approximation of the collisional operator which we would like to discuss in this report along with the details of implementation.

2. THE FOKKER–PLANCK OPERATOR

We consider characteristic time scales much longer then gyroperiod and characteristic spatial scales much larger than gyroradius of the particles. Under these conditions the kinetic equation reduces to the so-called guiding center approximation which allows us to exclude

azimuthal angle dependence in the kinetic equation [4]

$$\frac{\partial f^\alpha}{\partial t} + \xi v \frac{\partial f^\alpha}{\partial s} - v \frac{1-\xi^2}{2} \frac{\partial \ln B}{\partial s} \frac{\partial f^\alpha}{\partial \xi} = \hat{L}(f^\alpha), \tag{1}$$

where distribution function $f^\alpha(v, \xi, s, t)$ of the plasma species α depends upon the velocity v, cosine of the pitch-angle ξ, spatial variable s along the magnetic field line with the strength B, as well as time t. The second term in the left hand side describes convection, and the third term is responsible for magnetic "focusing" in a nonhomogeneous magnetic field due to the conservation of the magnetic moment, or the first adiabatic invariant of the particle. The operator in the right hand side includes terms in addition to the simple transport effects. In the present paper we will consider in detail only the coulomb collisional operator in its exact form as derived in [17].

Equation (1) can be transformed into the conservation form by the change of dependent variable according to $f^\alpha = F^\alpha B$

$$\frac{\partial F^\alpha}{\partial t} + \frac{\partial}{\partial s}(\xi v F^\alpha) - \frac{\partial}{\partial \xi}\left(v \frac{1-\xi^2}{2} \frac{\partial \ln B}{\partial s} F^\alpha \right) = \frac{1}{B} \hat{L}(F^\alpha B). \tag{2}$$

Here we took into account that the collsional operator $\hat{L}$ is the quadratic functional of the distribution function.

The expression for the coulomb collisional operator in the appropriate variables was given in [17]. We will use it in its equivalent conservation form as

$$\begin{aligned} \frac{1}{\Gamma_\alpha} \hat{L}(f^\alpha) = {} & \frac{1}{v^2} \frac{\partial}{\partial v} v^2 \left[D_{vv} \frac{\partial f^\alpha}{\partial v} + D_v f^\alpha + D_{v\xi} \frac{\partial f^\alpha}{\partial \xi} \right] \\ & + \frac{\partial}{\partial \xi} \left[D_{\xi\xi} \frac{\partial f^\alpha}{\partial \xi} + D_\xi f^\alpha + D_{\xi v} \frac{\partial f^\alpha}{\partial v} \right]. \end{aligned} \tag{3}$$

Here, collisional strength is defined by

$$\Gamma_\alpha = \frac{4\pi Z_\alpha^4 e^4}{m_\alpha^2} \tag{4}$$

and Fokker–Planck coefficients can be expressed as

$$D_{vv} = \frac{1}{2} \frac{\partial^2 G^\alpha}{\partial v^2} \tag{5}$$

$$D_v = \frac{1}{2} \frac{\partial}{\partial v} \left[\frac{1}{v^2} \frac{\partial}{\partial v} v^2 \frac{\partial G^\alpha}{\partial v} + \frac{1}{v^2} \frac{\partial}{\partial \xi} (1-\xi^2) \frac{\partial G^\alpha}{\partial \xi} - 2\tilde{H}^\alpha \right] \tag{6}$$

$$D_{v\xi} = D_{\xi v} = \frac{1-\xi^2}{2v^2} \frac{\partial^2}{\partial \xi \partial v} \frac{G^\alpha}{v} \tag{7}$$

$$D_{\xi\xi} = \frac{1-\xi^2}{2v^2} \left[\frac{(1-\xi^2)}{v^2} \frac{\partial^2 G^\alpha}{\partial \xi^2} + \frac{1}{v} \frac{\partial G^\alpha}{\partial v} - \frac{\xi}{v^2} \frac{\partial G^\alpha}{\partial \xi} \right] \tag{8}$$

$$D_\xi = \frac{(1-\xi^2)}{2v^2} \frac{\partial}{\partial \xi} \left[\frac{1}{v^2} \frac{\partial}{\partial v} v^2 \frac{\partial G^\alpha}{\partial v} + \frac{1}{v^2} \frac{\partial}{\partial \xi} (1-\xi^2) \frac{\partial G^\alpha}{\partial \xi} - 2\tilde{H}^\alpha \right] \tag{9}$$

using Rosenbluth's potentials $g^\alpha(\mathbf{v})$ and $h^\alpha(\mathbf{v})$

$$G^\alpha(\mathbf{v}) = \sum_\beta \frac{Z_\beta^2}{Z_\alpha^2} \ln \Lambda_{\alpha\beta} g^\beta(\mathbf{v}) \tag{10}$$

$$g^\beta(\mathbf{v}) = \int d^3\mathbf{v}' f^\beta(\mathbf{v}')|\mathbf{v} - \mathbf{v}'| \tag{11}$$

$$\tilde{H}^\alpha(\mathbf{v}) = \sum_\beta \frac{m_\alpha + m_\beta}{m_\beta} \frac{Z_\beta^2}{Z_\alpha^2} \ln \Lambda_{\alpha\beta} h^\beta(\mathbf{v}) \tag{12}$$

$$h^\beta(\mathbf{v}) = \int d^3\mathbf{v}' f^\beta(\mathbf{v}')|\mathbf{v} - \mathbf{v}'|^{-1}. \tag{13}$$

The Rosenbluth's potentials integral definitions (11) and (13) are equivalent to the Poisson problems

$$\Delta_v g^\beta = 2h^\beta, \qquad \Delta_v h^\beta = -4\pi f^\beta \tag{14}$$

with the distribution function serving as a source. In spherical velocity coordinates the Laplacian is

$$\Delta = \frac{1}{v^2}\frac{\partial}{\partial v} v^2 \frac{\partial}{\partial v} + \frac{1}{v^2}\frac{\partial}{\partial \xi}(1 - \xi^2)\frac{\partial}{\partial \xi}.$$

Thus the differential representation (14) immediately shows partial cancellation of terms in (6) and (9) where only

$$H^\alpha(\mathbf{v}) = \sum_\beta \frac{m_\alpha}{m_\beta} \frac{Z_\beta^2}{Z_\alpha^2} \ln \Lambda_{\alpha\beta} h^\beta(\mathbf{v})$$

will appear in coefficients D_v and D_ξ

$$D_v = -\frac{\partial H^\alpha}{\partial v}, \qquad D_\xi = -\frac{1 - \xi^2}{v^2}\frac{\partial H^\alpha}{\partial \xi}. \tag{15}$$

In fact the most complicated entries of the Fokker–Planck coefficients have been reduced to a simple functional of potential H^α only. Thus "friction" in velocity space has a relatively simple form in terms of Rosenbluth potentials. This fact for instance has been overlooked in [12], in their finite difference implementation of the Coulomb collisional operator. Simplification is considerable and obviously helps to avoid quite a large amount of unnecessary extra calculations. Moreover, the error of nonperfect numerical cancellation can potentially contribute to the round-off error buildup in the algorithm.

Equation (1) for each species has to be solved together with initial conditions

$$f^\alpha(s, v, \xi, t = 0) = \Psi_0^\alpha(s, v, \xi) \tag{16}$$

and is subject to boundary conditions at magnetically conjugate points in the atmosphere where the main source of energetic photoelectrons is operating

$$f^\alpha(s = -S, v, \xi, t) = \Psi_+^\alpha(v, \xi, t), \qquad \text{if } \xi > 0; \tag{17}$$

$$f^\alpha(s = +S, v, \xi, t) = \Psi_-^\alpha(v, \xi, t), \qquad \text{if } \xi < 0. \tag{18}$$

We choose some characteristic velocity of the problem $2V$, which normally will be equal to the highest velocity of the particle used in simulations on a bounded interval, so that $v \in [0, 2V]$. The characteristic spatial length is natural to set equal to the length $2S$ of the magnetic tube line from one hemisphere to another, from $-S$ to S. This choice defines the characteristic time of the problem τ as

$$\tau = \frac{2S}{2V}.$$

We change to dimensionless variables in (1)

$$t \to \frac{t}{\tau}, \qquad v \to \frac{v}{V} - 1, \qquad s \to \frac{s}{S}.$$

This particular scaling is motivated by the spectral collocation method we use for discretization of the problem in s, v, and ξ, which we describe in some detail in the next section.

Equation (1) is approximated by the spectral collocation method [7].

2.1. *Spectral Collocation*

The physical domain is mapped into $[-1, 1]$, the region where normally bounded orthogonal polynomials are defined. The set of orthogonal polynomials is chosen [7, 3]. We will be using Legendre polynomials $L_n(x)$ simply because the pitch angle variable is treated in a more simple way in the Coulomb collisional operator in that case. Other sets can be used for spatial and velocity variables. The grid is defined at the so-called Gauss–Lobatto points. Given a degree of the approximating polynomial N the Gauss–Lobatto points η_i for $i = 0 \ldots N$ are defined as $N - 1$ zeros of the derivative of $L_N(x)$ plus two end points -1 and 1.

Function $p(x)$ is approximated as the Nth order polynomial

$$p(x) = \sum_{k=0}^{N} c_k L_k(x). \tag{19}$$

The c_k's are called the Fourier coefficients of $p(x)$ with respect to the orthogonal basis $L_k(x)$. If we know the function's values $p_i = p(\eta_i)$ at the Gauss–Lobatto points, there is a one-to-one correspondence between the set of c_i and p_i. The Gauss–Lobatto weights w_i can be defined to approximate the integral

$$\int_{-1}^{1} p(x)\, dx = \sum_{j=0}^{N} p_j w_j. \tag{20}$$

This is the well known Nth order Gaussian quadrature formula. The important fact about this approximation can be proved: formula (20) is true (exact) for any polynomial $p(x)$ of the order less than $2N - 1$.

This formula is the basis for high accuracy numerical integration and is widely used in numerical computations. The formula (20) can be used for computing Rosenbluth potentials.

For differential equations approximation a similar high accuracy representation for the derivative can be obtained. From (19)

$$p' = \sum_{k=0}^{N} c_k L_k' = \sum_{k=0}^{N} c_k^{(1)} L_k. \tag{21}$$

This can be transformed into physical space in the form

$$p'(\eta_i) = \sum_{j=0}^{N} d_{ij}\, p(\eta_j). \tag{22}$$

Thus the derivative operator in the vector space p_k is equivalent to matrix multiplication. Derivative matrix entries d_{ij} are completely defined by the type and degree of orthogonal polynomial. It is important that formula (22) gives exact derivatives at the node points for any $p(x)$ which is a polynomial of degree less than N.

Using (22) on the nonuniform grid defined by Gauss–Lobatto points we can construct high accuracy approximation for integro-differential operators. The resulting linear system is dense. As a result direct (LU decomposition) or iterative methods must be used for solving the system of equations for p_k's. However, due to the relative high accuracy of the approximation the number of nodes can be significantly reduced in comparison to the conventional finite difference methods.

The Gauss–Lobatto grid has a nice property for our problem: it is denser to the ends of the interval, at $|x| = 1$, where in the case of the pitch angle we expect the distribution function of untrapped particles to concentrate due to the highly nonuniform magnetic field. In the case of the spatial variable along the magnetic field tube, grid points tend to concentrate at the lower altitudes, where most of the interesting physics is happening.

The common problem for the spectral method is due to the fact that discontinuous functions in general are poorly represented by the truncated Fourier series (19). This property is known as a Gibbs phenomenon: oscillations amplitude of the approximating polynomial in the neighborhood of the point of discontinuity stays bounded; it does not decrease as N increases. This problem is not serious for the parabolic systems which normally tend to produce smooth solutions even for initially discontinuous functions. It was shown that even for hyperbolic systems the Gibbs phenomenon is not a matter of great concern. It does not the change the dynamics of the solution but is a result of an attempt to accurately represent discontinuity at the given discretization level. Discontinuity is represented by the two–three points on the grid and is much better resolved than by normal finite difference (FD) schemes [12]. The FD approximations tend to introduce numerical diffusion and viscosity which has an irreversible effect on the long-term solution.

The Gibbs phenomenon can be excluded from the solution for cosmetic purposes of the final solution for better visualization of the result, or it can be done all the way along the solution process. The natural way to do this is to filter out the aliased high harmonics of the solution. Note however that sometimes this can have an undesirable effect. As a result of filtering not only the oscillation amplitude is reduced but also the width of the discontinuity is increased. Thus, for the problems where true location of the discontinuity and the effects of the width of the transition are important it may be important to keep all frequency spectra unchanged.

2.2. *Time Discretization*

For the time discretization, the time splitting or fractional steps method [16] is used. We discretize each operator in space, pitch angle, and particle velocity separately and for each time step advance distribution function in time using a separate operator sequentially. This modularized approach is very flexible in the sense of adding new physics into the system. The main disadvantage is that even if each operator separately is approximated by a stable scheme, we cannot allow very large time steps. Only in the limit of small time steps one can expect that results of sequential time steps to be close to the actual evolution of the system. In the case of nonlinear problems, as in the approximation of the Coulomb collisional operator, large time steps can even destabilize the resulting scheme. This disadvantage in our approach is greatly compensated for by the high accuracy approximation of all the operators involved.

One full time step includes four operations: calculation of the current values for the Fokker–Planck coefficients and three ADI steps accounting for evolution in space, velocity, and angle variables. We give details of implementation for each step below.

2.2.1. Calculation of Fokker–Planck coefficients. For evaluation of the diffusion coefficients as suggested in [17] we use expansion in terms of Legendre polynomials in the pitch angle variable

$$f^{\alpha}(v,\xi) = \sum_{n=0}^{\infty} f_n(v) P_n(\xi), \tag{23}$$

$$g(v,\xi) = \sum_{n=0}^{\infty} g_n(v) P_n(\xi), \tag{24}$$

$$h(v,\xi) = \sum_{n=0}^{\infty} h_n(v) P_n(\xi). \tag{25}$$

Calculation of spectral coefficients in (23)

$$f_n(v) = \frac{2n+1}{2} \int_{-1}^{1} f^{\alpha}(v,\xi) P_n(\xi)\, d\xi \tag{26}$$

takes advantage of high accuracy Guass–Lobatto quadrature according to (20).

After using identity (27)

$$\frac{d}{d\xi}(1-\xi^2)\frac{dP_n(\xi)}{d\xi} + n(n+1)P_n(\xi) = 0, \tag{27}$$

the Poisson equations (11) and (13) and the boundary conditions become

$$\begin{aligned} \frac{\partial}{\partial v} v^2 \frac{\partial h_n}{\partial v} - n(n-1)h_h &= -f_n, \\ \left.\frac{\partial h_n}{\partial v}\right|_{v=0} &= 0, \\ h_0(v=0) &= \int_0^{\infty} f(u) u\, du, \\ h_n(v=0) &= 0, \qquad \text{if} \quad n \neq 0 \end{aligned} \tag{28}$$

$$\begin{aligned} \frac{\partial}{\partial v} v^2 \frac{\partial g_n}{\partial v} - n(n-1) g_h &= 2h_n \\ \left. \frac{\partial g_n}{\partial v} \right|_{v=0} &= 0, \\ g_0(v=0) &= \int_0^\infty f(u) u^3 \, du, \\ g_n(v=0) &= 0, \qquad \text{if } n \neq 0. \end{aligned} \tag{29}$$

These equations can be solved analytically using Green's function of the linear differential operator in (27) and (28) as suggested in [17], and this procedure was followed in finite difference implementation [12]

$$h_n(v) = \frac{4\pi}{2n+1} \left[\int_0^v du f_n(u) \frac{u^{n+2}}{v^{n+1}} + \int_v^\infty du f_n(u) \frac{v^n}{u^{n-1}} \right] \tag{30}$$

$$\begin{aligned} g_n(v) = \frac{4\pi}{1-4n^2} \Bigg[& \int_0^v du f_n(u) \frac{u^{n+2}}{v^{n-1}} \left(1 - \frac{2n-1}{2n+3} \frac{u^2}{v^2} \right) \\ & + \int_v^\infty du f_n(u) \frac{v^n}{u^{n-3}} \left(1 - \frac{2n-1}{2n+3} \frac{v^2}{u^2} \right) \Bigg]. \end{aligned} \tag{31}$$

The numerical evaluation of the Rosenbluth potentials h_n and g_n according to Green's function solutions (30) and (31), however, bears a large numerical error. This can be clearly seen, for example, in the case $n = 0$ when h_0 degenerates into a one-sided indefinite integral from $u = 0$ to $u = v$ and for small v only very few points on the grid are used for evaluation of the integral. As a result high order Gaussian quadrature formulas become unusable and lower order integration schemes lead to the lose of spectral accuracy provided by spectral collocation. Therefore, instead of numerical evaluation of integrals (30) and (31), we solve directly boundary value problems (28) and (29) by the spectral collocation method, which ensures spectral accuracy. In terms of efficiency of calculations in the case of solving (28) and (29) by direct matrix inversion, the number of arithmetic operations is of the same order as numerical quadrature for evaluation of integrals (30) and (31). There are also potentially more efficient methods for solving differential equations (28) and (29); for example, iterative methods can be much more efficient on large grids. At the present time only a direct solution (by LU decomposition) has been implemented.

In our algorithm the differential operator in the left hand sides of (28) and (29) including the boundary conditions is approximated as a matrix multiplication operator using the spectral collocation method described above. The inverse of the matrix is calculated at the initialization stage of the program and stored in the memory. Thus the calculation of the spectral coefficients of the Rosenbluth potentials requires only matrix multiplication for each harmonic n. In order to obtain the Fokker–Planck coefficients according to (5), (7), (8), (15) the differentiation over velocity v is done numerically using the spectral collocation derivative matrix. The differentiation over velocity can be done before or after the calculation of the inverse Legendre transform according to (23). Clearly it is more efficient to differentiate the potential once in velocity space, rather than to perform n differentiations of the spectral coefficients g_n. As for the differentiation in ξ, this can be done analytically before the inverse transform using the properties of the Legendre polynomials given by (27)

and

$$(1-\xi^2)\frac{dP_n(\xi)}{d\xi} = \frac{n(n+1)}{2n+1}\left(P_{n-1}(\xi) - \xi P_{n+1}(\xi)\right), \tag{32}$$

and

$$(2n+1)\xi P_n(\xi) = (n+1)P_{n+1}(\xi) + nP_{n-1}(\xi). \tag{33}$$

This step again avoids extra computational effort related to the numerical differentiation of the Fokker–Planck coefficients with respect to ξ in the algorithm. The numerical implementation demonstrated that this procedure gives a highly accurate representation of the Fokker–Planck coefficients.

The update of the coulomb collision Fokker–Planck coefficients using current values for the distribution function is one of the most computationally intensive parts of the algorithm. The whole procedure however is nonrecursive and all stages are basically represented as a matrix multiplication. This makes the algorithm highly vectorizable.

In the simplest time factorization scheme these coefficients are used throughout all the fractional time steps. This is justified by the observation that normally diffusion coefficients change much slower than the distribution function itself [13]. This limitation is dictated by the high computational cost of the diffusion coefficients evaluation.

2.3. *Alternating Direction Implicit Time Splitting*

Next, using calculated diffusion coefficients we construct implicit approximations to the problem

$$\frac{1}{\gamma^\alpha}\frac{\partial f^\alpha}{\partial t} = \frac{1}{v^2}\frac{\partial}{\partial v}v^2\left[D_{vv}\frac{\partial f^\alpha}{\partial v} + D_v f^\alpha\right] + \frac{\partial}{\partial \xi}\left[D_{\xi\xi}\frac{\partial f^\alpha}{\partial \xi} + D_\xi f^\alpha\right] + \frac{1}{v^2}\frac{\partial}{\partial v}\left[v^2 D_{v\xi}\frac{\partial f^\alpha}{\partial \xi}\right] + \frac{\partial}{\partial \xi}\left[D_{\xi v}\frac{\partial f^\alpha}{\partial v}\right]. \tag{34}$$

The dimensionless factor γ^α gives the value of the the relative strength of the collisions in the dimensionless form,

$$\gamma^\alpha = \frac{4\pi Z_\alpha^4 e^4 n_\alpha S}{m_\alpha^2 (2V)^4}, \tag{35}$$

where n_α is the density of the particles. All derivative operators in (34) are represented in a matrix form and the complete operator in the right hand side is described by the four matrices D^v, D^ξ, $D^{\xi v}$, and $D^{v\xi}$, where for instance $V \times V$ matrix D^v_{ij} is given by

$$D^v_{ij}(\xi_l) = \sum_{k=0}^{V} d^v_{ik} d^v_{kj} \frac{v_k^2}{v_i^2} D_{vv}(v_k, \xi_l) + d^v_{ij}\frac{v_j^2}{v_i^2} D_v(v_j, \xi_l)$$

and $X \times X$ matrix D^ξ_{ij} is

$$D^\xi_{ij}(v_l) = \sum_{k=0}^{X} d^\xi_{ik} d^\xi_{kj} D_{\xi\xi}(v_l, \xi_k) + d^\xi_{ij} D_\xi(v_l, \xi_j)$$

with d^v_{ik} and d^ξ_{ik} representing the corresponding derivative collocation matrix defined in (22). V and X represent the number of collocation points in velocity and angle variables. The mixed derivative term however will always be represented in explicit form

$$\sum_{k=0}^{V}\sum_{l=0}^{X} d^v_{ik} d^\xi_{jl}\left[D_{\xi v}(v_i,\xi_l)+\frac{v_k^2}{v_i^2}D_{v\xi}(v_k,\xi_l)\right] f^{(n)}_{kl},$$

where we dropped index numbering plasma species here, and f^n_{ij} is the value of the distribution function at time labeled n and ith collocation point along the velocity, and jth collocation point along the angle variable ξ,

$$f^{(n)}_{ij} = f(t=t_n, v=v_i, \xi=\xi_j).$$

This explicit representation in the cases where large derivatives occur during the evolution of the plasma can potentially lead to numerical instabilities [18]. In such cases different representations may be required with an appropriate preconditioner matrix.

Using the above matrix representation of the kinetic equation we construct a two-step implicit scheme for updating vector $f^n_{v\xi}$ to the next fractional time step f^{n+1}_{ij}. First an ADI (alternating direction implicit) step implicitly accounts for velocity derivatives

$$\begin{aligned} f^{(n+1/2)}_{ij} &- \frac{\gamma\tau}{2}\sum_{k=0}^{V} D^v_{ik}(v_k,\xi_j)\, f^{(n+1/2)}_{kj} \\ &= f^{(n)}_{ij} + \frac{\gamma\tau}{2}\left[\sum_{k=0}^{X} D^\xi_{ik}(v_i,\xi_k)\, f^n_{ik} \right. \\ &\quad \left. + \sum_{k=0}^{V}\sum_{l=0}^{X} d^v_{ik} d^\xi_{jl}\left[D_{\xi v}(v_i,\xi_l)+\frac{v_k^2}{v_i^2}D_{v\xi}(v_k,\xi_l)\right] f^{(n)}_{kl}\right] \end{aligned} \tag{36}$$

and the second step implicitly accounts for angle derivatives

$$\begin{aligned} f^{n+1}_{ij} &- \frac{\gamma\tau}{2}\sum_{k=0}^{X} D^\xi_{jk}(v_i,\xi_k)\, f^{n+1}_{ik} \\ &= f^{n+1/2}_{ij} + \frac{\gamma\tau}{2}\left[\sum_{k=0}^{V} D^\xi_{jk}(v_i,\xi_k)\, f^{n+1/2}_{ik} \right. \\ &\quad \left. + \sum_{k=0}^{V}\sum_{l=0}^{X} d^v_{ik} d^\xi_{jl}\left[D_{\xi v}(v_i,\xi_l)+\frac{v_k^2}{v_i^2}D_{v\xi}(v_k,\xi_l)\right] f^{(n+1/2)}_{kl}\right]. \end{aligned} \tag{37}$$

These two equations are in the form of linear algebraic systems

$$\sum_{j=0}^{V} A_{ij}\, f^{n+p}_{jl} = \sum_{j=0}^{V} B_{lij}\left(f^{(n+p-1/2)}_{ij}\right), \qquad \text{for } p = 1/2, 1. \tag{38}$$

Matrix inversion is the most computationally complex part of the code, which in general requires N^3 operations for $N \times N$ matrix. For sparse grids, with the number of collocation

points less than 100, Eq. (38) can be efficiently solved by the direct inversion method. For larger number of collocation points, iterative methods of solution are more efficient. In that case it is more appropriate to combine velocity and angle fractional steps into one step. This has the advantage of allowing implicit representation for mixed derivative terms. The work on development of iterative solvers with appropriate preconditioners for the Fokker–Planck equation with the Coulomb collisional operator is planned for the near future.

The order of approximation in velocity variables is spectral, higher than the number of grid points. Practically the accuracy of approximation is limited only by round-off computational errors. Therefore the first-order finite-difference approximation in time of the ADI method is the limiting factor for overall accuracy of the method.

Matrix A_{ij} also accounts for boundary conditions. For instance, on the first fractional time step the boundary condition

$$\frac{\partial f}{\partial v} = 0, \qquad \text{at } v = 0$$

is enforced. In terms of the collocation derivative this condition becomes

$$\sum_{j=0}^{N} d^v_{0j} f_{ij} = 0,$$

where d^v_{ij} is a first derivative matrix for the velocity variable. Thus in order to account for the boundary condition we just replace the entries in the matrix A_{0j} (which are in fact singular) by d_{0j} and the right hand side by 0. Note how naturally the spectral collocation method treats the boundary condition.

Moreover, the conservation laws can be enforced in the solution. For instance, Eq. (34) conserves particle density or the integral

$$\int_0^\infty f(u) u^2 \, du = \text{ const.}$$

This can be approximated as

$$\sum_{j=0}^{N} w_j f_j^{n+p} v_j^2 = \sum_{j=0}^{N} w_j f_j^{n+p-1/2} v_j^2$$

in the case when the distribution function does not depend on the angle variable. We can enforce the conservation law by again replacing one of the rows, let's say the kth row, of matrix A_{kj} with $w_j v_j^2$ and the right hand side then is replaced by

$$\sum_{j=0}^{N} w_j f_j^n v_j^2.$$

The appropriate place for such replacement is at the lower velocity end, i.e., at small values of k. The distribution function is large there and also collocation points are more dense on the grid. Therefore, the necessary correction to the solution is affected with smallest relative change of the solution. In general, this procedure is not required for the spectral collocation method. However, we use it as an additional testing tool in one-dimensional problems.

When matrix A_{ij} has been constructed, system (38) is being solved by LU decomposition. Similarly the boundary conditions for the second fractional step (36) are enforced

$$\frac{\partial f}{\partial \xi} = 0, \qquad \text{at } v = 0.$$

2.3.1. Fractional time step accounting for spatial convection. In an exactly similar way the optional spatial derivative term can be added. The corresponding operator again can be represented in matrix form using derivative matrix d^s_{ij} defined on the collocation grid along the spatial coordinate,

$$D^s_{ij}(v_l, \xi_m) = \xi_m v_l d^s_{ij} \tag{39}$$

with the boundary conditions specified at $s = -1$ and $s = 1$. Using this matrix representation the third fractional step is added with implicit inclusion of the spatial derivative and explicit account of remaining operators in v and ξ. Explicit contribution of the spatial derivative should also be added to the previous fractional steps.

3. NUMERICAL RESULTS

We applied the spectral collocation method to a couple of simple but interesting problems in order to test the algorithm. The code was implemented in C++ and run on a Pentium 200 MHz computer. Average time required for performing one fractional time step in velocity space on the grid with 33 collocation points was of the order of 100 s. The numerical complexity of the code is determined by matrix inversion at the cost N^3. For the sparse grid used in the tests this does not represent a technical problem. For grids larger than $\approx$50 the iterative solution techniques will reduce computational cost considerably.

3.1. *Is the Overrelaxation Real?*

As a first application of the spectral collocation code for (1) with exact collisional operator we solved the problem of relaxation of the distribution function which at $t = 0$ is close to the delta function in the velocity variable, as in [15]. Apart from giving a clear opportunity for testing the algorithm this particular problem has been reported to have a rather interesting property. In [15] the relaxation of the initial distribution in the spherically symmetric case exhibited the "overrelaxation" of the distribution function in the vicinity of $v = 0$. By overrelaxation we mean that the distribution function at $v = 0$ became larger than the corresponding equilibrium stationary Maxwellian distribution. However, the final stage, true equilibrium, was not reproduced in [15]. The reason for that is not specified in the paper. The absence of overrelaxation in fact has been reported earlier, for example, in [1].

We let the initial distribution take exactly the same form as in [15]

$$f(v) = \exp(-10(v/0.3 - 1)^2)$$

and followed the evolution of the distribution function in time. Initially the relaxation character was quite similar to that reported in [15], see Fig. 1; however, the "overrelaxation" phenomenon was not observed, as it is clear from the time profile of the distribution function value at $v = 0$ in Fig. 2. Instead, the distribution function monotonically approached equilibrium Maxwellian everywhere in velocity space. It should be noted that in this calculations we enforced density conservation in the algorithm.

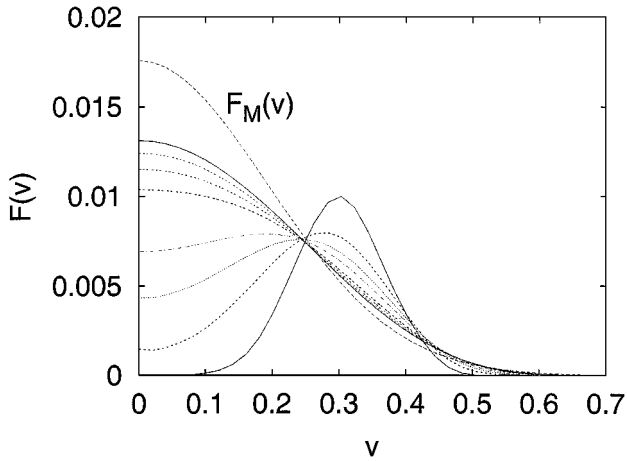

FIG. 1. The evolution of the initial distribution function shown with time steps 20 in dimensionless units. It can be seen as evolution enters a very slow phase after a period of relatively fast relaxation.

This result is in good agreement with finite-difference calculations of [1]. Special attention in this work has been paid to ensure monotonicity of the entropy decay. In order to check how this property is accounted for by the spectral collocation code we plot the evolution of the entropy functional

$$H = \int_0^\infty f(v) \ln f(v) v^2 \, dv$$

in Fig. 3. As expected, entropy is a smooth decreasing function of time and is in good agreement with calculations in [1].

We tried to implement for spherically symmetric problem (1) the explicit algorithm outlined in [15] and also failed to reproduce the overrelaxation phenomenon. In addition to being extremely slow because of the stability condition imposed by the explicit scheme, numerical results show that the density starts to accumulate at the times corresponding to the

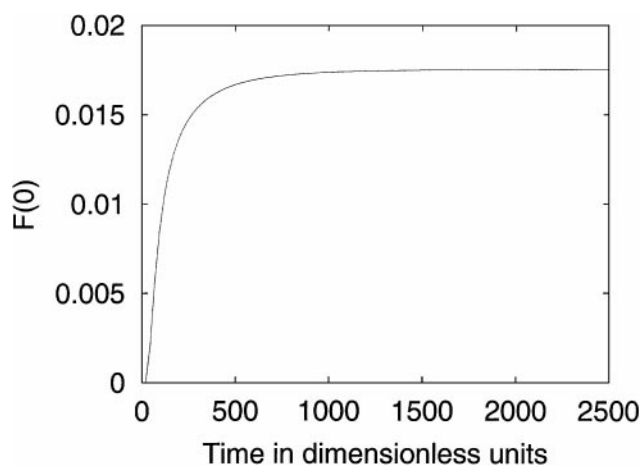

FIG. 2. The evolution of the distribution function value at $v = 0$ clearly demonstrates the monotonic behavior with no sign of the overrelaxation at small velocities.

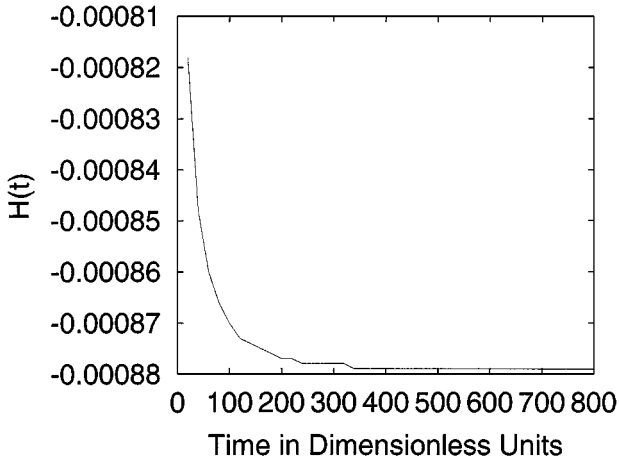

FIG. 3. The evolution of the entropy functional $H(t)$ in time.

overrelaxation appearance. The typical number of time step required to follow the evolution of the distribution function up to the times when distribution approaches Maxwellian as dictated by the stability condition of the explicit scheme is large, of the order of 10^6. Thus it is natural to suggest that the overrelaxation seen in the explicit algorithm can be caused by numerical accumulation of the error of the approximation of the density and energy integrals of the system. Note that we were not able to reproduce exactly the algorithm used in [15] because some details of the implementation are not given in the paper, such as the way in which the boundary conditions where implemented.

Our implicit algorithm is not sensitive to the value of the time step τ. The stationary distribution, at time $t = 2500$, is very close to Maxwellian, as can be seen in Fig. 4, where the difference between the distribution function and the corresponding Maxwellian (for the same density and energy of the distribution) is plotted. This plot also shows that the difference between the Maxwellian and relaxed distribution has not yet completely vanished;

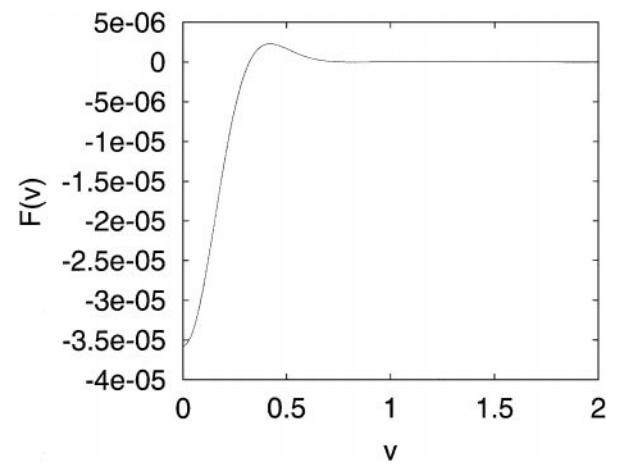

FIG. 4. The difference between the distribution function at time $t = 2500$ and a true stationary Maxwellian solution shows that relaxed distribution very slowly approaches the stationary solution.

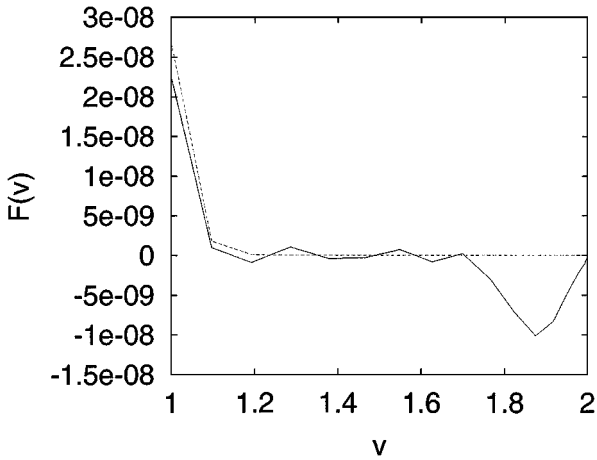

FIG. 5. The high energy end of the distribution function at time $t = 2500$ and true stationary Maxwellian solution shows that the high energy part is not resolved by the spectral collocation.

there are still less particles in the region of small velocities and some overabundance of particles is still present at the location of the initial distribution function, $v = 0.3$.

The results indeed reveal a very high accuracy of the spectral collocation. Note that these are results of the integration of the time dependent problem with relatively large time step $\tau = 0.1$ with a 33-point grid, or $\Delta v = 0.06$ for an equivalent finite difference spatial step. However, there is a limitation. Figure 5 shows the high energy end of the relaxed distribution and corresponding Maxwellian. It is clear that the high energy part of the distribution is in fact not resolved. Although the absolute value of the error is of the order of machine precision, the relative error is large and leads to significant loss at high energies. This is because of the global nature of the spectral methods in general: all available information, the distribution function at all collocation points, is used to approximate derivatives and integrals of the distribution function at any given point. As a result the same numerical error applies to the regions where the distribution function is very small and to the regions where the distribution function is large. Thus in order to increase the resolution of the distribution function where it is small in magnitude one has to decrease the computational round off errors, i.e., increase the precision of floating point numbers used in calculations. Another solution of this problem can be attempted when some additional information is available. For instance in this simple relaxation problem the density and temperature of the distribution are constant and this can be used to factor out the exponential dependence at large energies. This approach naturally suggests the use of Laguerre polynomials as a basis for orthogonal expansion and collocation. In addition to providing more uniform approximation this approach also allows us to define the grid in energy corresponding to the semi-infinite region, as Laguerre polynomials are defined on the semi-infinite interval [7, 9]. There are, however, additional technical problems arising in numerical evaluations of the Laguerre polynomials [7] and for this reason we postponed research in this direction for the future.

3.2. *Superthermal Heating*

It is anticipated that the main application for a highly accurate Fokker–Planck equation solver will be in the area of interactions of the plasma with collective oscillations. The

self-consistent picture of the plasma waves and particles requires accurate modeling of the electromagnetic properties and the collisional effects in the plasma. One important type of such collective effects is a heating of the plasma as a result of interaction with nonthermal electromagnetic waves.

We have tested the spectral collocation algorithm on the simple case of plasma heating suggested in [8]. The superthermal radiation field is shown to enhance the diffusion coefficients in velocity space by the additive factor

$$A/v.$$

In [8] it was noted that this particular form when used in the linearized version of the Fokker–Planck equation (1) enforces the "stationary" solution which is a power-law distribution at large energies. Recently this same idea was exploited in [14] to show that the so-called kappa-distribution can be expected as a consequence of the turbulence of whistler type plasma waves.

However, as was pointed out in [9], the immediate consequence of the nonthermal diffusion is a heating of the distribution function. As a result no stationary solution exists and the long time evolution solution should rather be attempted in the form of a self-similar solution. It can be shown then that self-similar solution in fact is the exponential

$$\exp(-v^3)$$

for the particular form of the nonthermal diffusion coefficient suggested in [8]. The width of this distribution is increasing in time and as a result of the overall decrease of the total diffusion coefficient at large velocities, the high energy tail always remains undeveloped even in comparison to the Maxwellian distribution.

These aspects are clearly seen in the numerical results shown in Fig. 6. The initial distribution function is taken in the same form is in the previous test problem. The diffusion coefficient was augmented by the term $0.001/v$. After sufficient time the distribution function approaches the self-similar form. The Maxwellian distribution for the same density and energy content is also shown. Clearly the self-similar solution is not a Maxwellian.

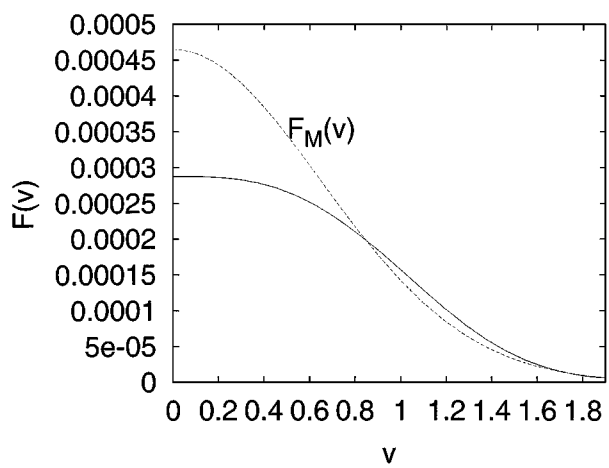

FIG. 6. As a result of the interaction with the nonthermal radiation field a self-similar solution is formed which is quite different from Maxwellian.

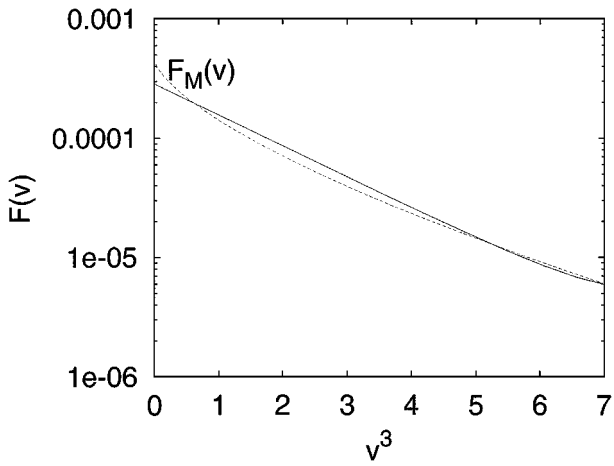

FIG. 7. Using the logarithmic plot against v^3 we clearly see that the self-similar asymptotic solution is indeed very close to the scaling given by the analytical solution $\exp(-v^3)$.

The logarithmic plot against v^3 in Fig. 7 shows that the self-similar solution is very close to $\exp(-v^3)$ scaling. There is no doubt that the power-law distribution cannot be produced by simple nonthermal diffusion. In order to force the power-law solution in the system with nonthermal diffusion the minimum requirement is to provide the energy loss somehow at exactly the same overall rate as heating but differently distributed over the velocity space. The problem then becomes similar to the determination of energy cascade with Kolmogoroff–Obukhof type spectra.

4. CONCLUSIONS

The first test results of the implementation of a high accuracy spectral collocation method for the kinetic equation with the exact coulomb collisional operator were presented. The implementation of the exact collisional operator in a spectral collocation algorithm is straightforward. On the strong side the ability to incorporate the conservation properties of the operator directly into the algorithm should be mentioned. This considerably increases reliability of the results as it addresses the most important properties of the system, as conservation of the particle density and energy, from the physical point of view.

The high order spectral collocation approximation of the integro-differential operators is global. The derivatives at any collocation point are estimated using not only a few closest points on the grid, as in conventional finite difference schemes, but also the information at all available collocation points is incorporated in the approximation. As a result, a highly accurate approximation is achieved everywhere on the grid. However, this is also the main drawback of the spectral collocation method. Because the approximation is uniform, the regions of the velocity space where the distribution function is exponentially small are used simultaneously with those from the regions where the distribution function is relatively large. When the difference in the magnitude of distribution function becomes larger than numerical precision of the computer the significance of the small values of the distribution function is lost. Thus normally it is not possible to describe by a simple spectral collocation method the distribution function variations of many orders of magnitude. In that case it is necessary to

factor globally the distribution function by an appropriate function. In most cases it should be sufficient to factor exponential dependence which implies that Laguerre polynomials in the energy of the particle represent an attractive choice of the orthogonal polynomial for the spectral collocation. In addition to properly accounting for the exponential decay of the distribution function at large energies, this choice also makes use of the unbounded semi-infinite domain in energy variable [9].

ACKNOWLEDGMENTS

This work was supported by the National Science Foundation under Contracts ATM-9710326, ATM-9896049, and NASA Contract NAG5-6976.

REFERENCES

1. C. Buet and S. Cordier, Conservative and entropy decaying numerical scheme for the isotropic Fokker–Planck–Landau operator, *J. Comput. Phys.* **145**, 228 (1998).
2. C. Buet, S. Cordier, P. Degond, and M Lemou, Fast algorithms for numerical, conservative, and entropy approximations of the Fokker–Planck–Landau equation, *J. Comput. Phys.* **133**, 310 (1997).
3. C. Canuto, M. Y. Hussaini, A. Quarteroni, and T. A. Zang, Spectral methods in fluid dynamics, in Springer Series in Computational Physics (Springer-Verlag, New York/Berlin, 1987).
4. G. F. Chew, M. L. Goldberger, and F. E. Low, The Boltzmann equation and the one-fluid hydromagnetic equations in the absence of particle collisions, *Proc. R. Soc. London Ser. A* **236**, 112 (1956).
5. P. Degond and B. Lucquin-Desreux, An entropy scheme for the Fokker–Planck collisions of the plasma kinetic theory, *Numer. Math.* **68**, 239 (1994).
6. E. Frenod and B. Lucquin-Desreux, On conservative and entropic discrete axisymmetric Fokker–Planck operators, M^2AN **33**, 307 (1998).
7. D. Funaro, Polynomial approximation of differential equations, in Lecture Notes in Physics (Springer-Verlag, New York/Berlin, 1992).
8. A. Hasegawa, K. Mima, and M. Duong-van, Plasma distribution function in a superthermal radiation field, *Phys. Rev. Lett.* **54**(24), 2608 (1985).
9. I. K. Khabibrakhmanov and D. Summers, Spectral representation of the Coulomb collisional operator, *J. Plasma Phys.* **58**(3), 475 (1997).
10. G. V. Khazanov, T. I. Gombosi, and A. F. Nagy, Analysis of the ionosphere-plasmasphere transport of superthermal electrons. 1. Transport in the plasmasphere, *J. Geophys. Res.* **97**(A11), 16,887 (1992).
11. G. V. Khazanov, T. Neubert, and G. D. Gefan, A unified theory of ionosphere-plasmasphere transport of suprathermal electrons, *IEEE Trans. Plasma Sci.* **22**(2), 187 (1994).
12. J. Killeen, A. A. Mirin, and M. E. Rensink, The solution of the kinetic equations for a multispecies plasma, in *Methods in Computational Physics* (Academic Press, New York/London, 1976), Vol. 16, p. 389.
13. S. Livi and E. Marsch, On the collisional relaxation of solar wind velocity distributions, *Ann. Geophys.* **4**(5), 333 (1986).
14. C.-Y Ma and D. Summers, Formation of the power-law energy spectra in space plasmas by stochastic acceleration due to whistler-mode waves, *Geophys. Res. Lett.* **25**, 4099 (1998).
15. W. M. MacDonald, M. N. Rosenbluth, and W. Chuck, Relaxation of a system of particles with Coulomb interactions, *Phys. Rev.* **107**, 350 (1957).
16. R. D. Richmyer and K. W. Morton, *Difference Methods for Initial-Value Problems*, 2nd ed., Interscience Tracts in pure and Applied Mathematics (Interscience/Wiley, New York, 1967).
17. M. N. Rosenbluth, W. M. MacDonald, and D. L. Judd, Fokker–Planck equation for an inverse-square force, *Phys. Rev.* **107**, 1 (1957).
18. F. S. Zaitsev, V. V. Longinov, M. R. O'Brien, and R. Tanner, Difference schemes for the time evolution of the three-dimensional kinetic equations, *J. Comput. Phys.* **147**, 239 (1998).